Proc. Indian Acad. Sci. (Earth Planet. Sci.), Vol. 99, No. 4, December 1990, pp. 681–692.

The nature of horizontal anomalies and magnetotelluric impedance over southern India

A K AGARWAL and J T WEAVER

Department of Physics and Astronomy, University of Victoria, Victoria, B. C., Canada, V8W 3P6

Abstract. The nature of horizontal anomalies and anomalous current systems in the region of the southern Indian peninsula is theoretically calculated with the aid of a thin sheet algorithm for northward and westward polarizations of a uniform inducing magnetic field of period 20 min. The numerical model of the geoelectric structure is the one devised by Agarwal and Weaver (1989). The model results indicate the correspondence between the general features of the computed horizontal anomalies and the observed anomalies both at temporary array stations and at two permanent magnetic observatories (ANN and TRD). On the basis of model estimates of apparent resistivity and phase it is suggested that a one-dimensional interpretation of the sub-surface conductivity structure is valid near two of the array stations, whereas at all other coastal and inland stations, two- or three-dimensional interpretations of magnetotelluric (MT) data are required.

Keywords. Horizontal anomalies; magnetotelluric impedance; anomalous current systems; equivalent current systems; apparent resistivity.

1. Introduction

Geomagnetic induction in southern India by both uniform and non-uniform sources has been a subject of considerable interest because of the presence of oceans on three sides of the peninsula, and also the proximity of the dip-equator (figure 1). Numerical model studies (Takeda and Maeda 1979; Ramaswamy *et al* 1985; Mareschal *et al* 1987; Agarwal and Weaver 1989) and analogue model studies (Papamastorakis and Haerendel 1983) have shown the importance of the Indo-Ceylonese graben in the Palk-Strait region in explaining the magnetic variation anomalies reported at three permanent equatorial stations Trivandrum (TRD), Kodaikanal (KOD) and Annamalainagar (ANN) by Srivastava and Sanker Narayan (1967), Nityananda *et al* (1977), Rajaram *et al* (1979) and Singh *et al* (1982). A recent analysis of magnetic data from two Sri Lankan stations Kondavil and Hikkaduwa (figure 1), provides further evidence in support of the Palk-Strait conductive graben (Kunaratnam 1987).

A study of temporary magnetic array data by Thakur *et al* (1986) indicated the existence of a deep-seated conductor of crustal origin across the Comorin ridge. The authors surmised that there is a likelihood of current concentration in the triple rift near TRD and the Palk-Strait postulated by Burke and Dewey (1973). It was proposed by Nityananda and Jayakumar (1981) that the enhanced electrical conductivity causing the geomagnetic anomalies, dierectly or indirectly, is related to the geology and tectonics of the region. These observations led Mareschal *et al* (1987) to investigate a thin-sheet numerical induction model of southern India which included a conductivity structure across the Comorin ridge as well as the Palk-Strait plus a

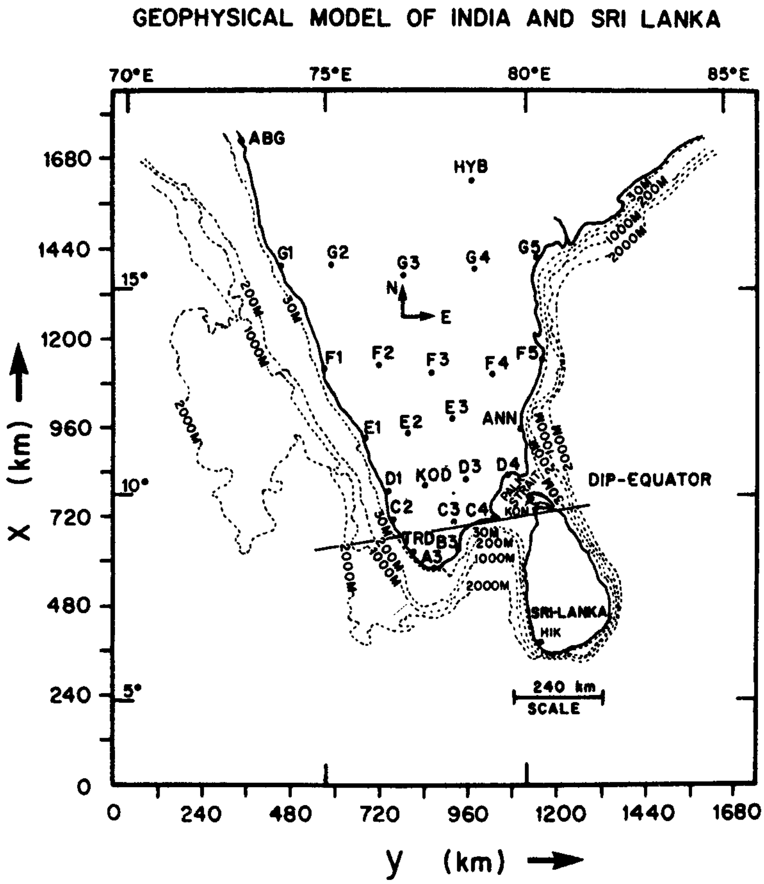

Figure 1. Map of the Indian peninsula and Sri Lanka showing the locations of the Southern array stations and the three permanent magnetic observatories ANN, KOD and TRD (after Agarwal and Weaver 1989). The position of two Sri Lankan stations Kondavil (KON) and Hikkaduwa (HIK) is also marked.

proposed western extension giving a progressive return to normal conductivity. The period of the magnetic variation was taken to be 108 min in their study. For the solution of the problem, they used the integral equation method of Vasseur and Weidelt (1977) which requires an integration only over the anomalous region, but suffers from the disadvantage that the region under investigation must be completely surrounded by an unrealistic uniform ocean. As a result, only three rows (B, C, D) of the southern array could be included in their model.

Recently, Agarwal and Weaver (1989) have also conducted a numerical study of induction around the Indian peninsula using the thin sheet algorithm of McKirdy *et al* (1985), and incorporating three subsurface conductors (i) in the Indo-Ceylon graben, (ii) underneath or nearby the Comorin ridge and (iii) along the west coast rift. They later extended their study to include source effects associated with the equatorial electrojets (Agarwal and Weaver 1990). This algorithm is more demanding on computer storage and CPU time but permits the model to approach a two-dimensional configuration at its boundaries. The anomalous electrical conductivity along the west coast was included in their model because the observed Z-variations along this coast could not be explained by the simple coast effect alone. The northward extent of this conductor appears to terminate somewhere between F1 and Alibag (ABG), the permanent magnetic station at which a negative Z variation is recorded in accordance with the coast effect (see Nityananda *et al* 1977). Since Ramaswamy *et al* (1985) have suggested that Z-variations near coastal stations will be associated with both the H- and D-components of the external magnetic field, numerical results were obtained for both a northwards (H) and westwards (D) polarization of the inducing field. Only short-period variations of period 20 min were considered; longer periods could not be handled by the algorithm.

In this paper we extend this earlier study by calculating the signatures of the horizontal magnetic anomalies and associated current systems. The computed values of the apparent resistivities and phases at each array station are also presented in the hope that they will be useful in future when MT measurements are taken over this zone. The numerical model of the geoelectric structure is shown in figure 2.

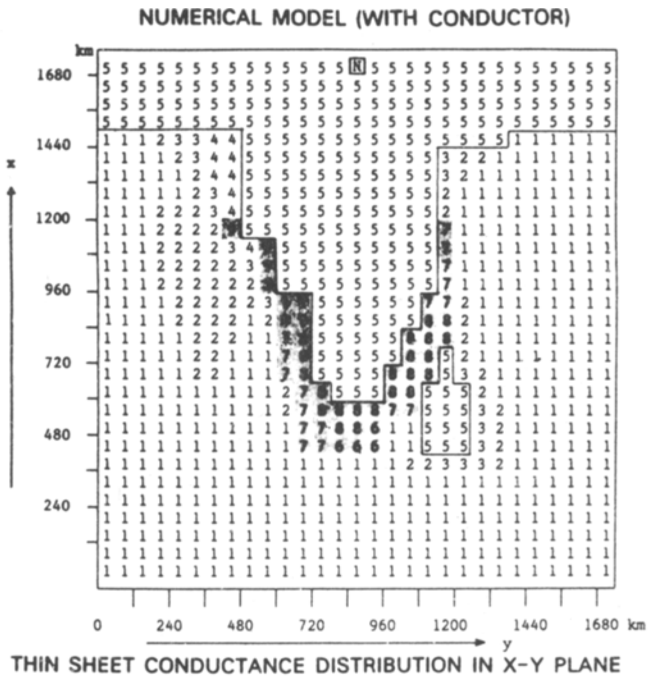

TWO LAYER MODEL

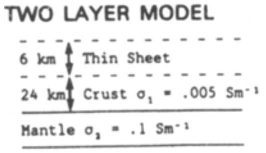

No.	Conductances (mhos)	Conductances (dimensionless)
1	8020	6.51 E + 00
2	6023	4.89 E + 00
3	2028	1.64 E + 00
4	829	6.73 E − 01
5	30	2.43 E − 02
6	21000	1.70 E + 01
7	19500	1.58 E + 01
8	16500	1.18 E + 01
9	8020	6.51 E + 00

Figure 2. Numerical model with lateral conductivity contrast due to land and the varying ocean depth from 200 m to 2000 m and the additional sub-surface conductors included in the Palk-Strait region, underneath or nearby the Comorin ridge and along the west coast rift (after Agarwal and Weaver 1989).

2. Calculated parameters

In this section we define the various parameters that are used to display the calculated effects of induction in our model of the Indian peninsula. As mentioned in the introduction we concentrate our attention particularly on parameters that represent the anomalous horizontal magnetic fields and the induced current systems.

2.1 *The horizontal disturbance vector*

Schmucker (1970 p. 20) suggested that a linear relationship exists between the anomalous horizontal components (H_a, D_a) arising from a lateral inhomogeneous structure and the normal horizontal components (H, D) due to the normal or host one-dimensional conductivity structure. In other words, assuming a time dependence $\exp(i\omega t)$ in all field vectors, we have

$$H_a = h_H H + h_D D,$$
$$D_a = d_H H + d_D D, \tag{1}$$

where h_H, h_D, d_H and d_D are the various (frequency-dependent) transfer functions. These transfer functions give rise to complex perturbation arrows $\mathbf{p}$ and $\mathbf{q}$ defined as

$$\mathbf{p} = h_H \hat{\mathbf{x}} + d_H \hat{\mathbf{y}},$$
$$\mathbf{q} = h_D \hat{\mathbf{x}} + d_D \hat{\mathbf{y}}, \tag{2}$$

where $\hat{\mathbf{x}}$ and $\hat{\mathbf{y}}$ are unit vectors directed northwards and eastwards respectively. It is easy to compute these arrows for each polarization by taking the regional magnetic field unity in dimensionless units. When the inducing magnetic field is directed northwards (i.e. $H = 1$, $D = 0$), the perturbation arrows will be

$$\mathbf{p} = H_a \hat{\mathbf{x}} + D_a \hat{\mathbf{y}}, \quad \mathbf{q} = 0, \tag{3}$$

where $H_a = H - 1$ and $D_a = D$. If the inducing field is directed westwards (i.e. $H = 0$, $D = -1$), the perturbation arrows will be

$$\mathbf{q} = -H_a \hat{\mathbf{x}} - D_a \hat{\mathbf{y}}, \quad \mathbf{p} = 0, \tag{4}$$

where $H_a = H$, $D_a = D + 1$. Thus the $\mathbf{p}$- and negative $\mathbf{q}$-vectors, for northward and westward polarizations respectively, define the horizontal disturbance magnetic field

$$\mathbf{B}_a = H_a \hat{\mathbf{x}} + D_a \hat{\mathbf{y}}. \tag{5}$$

An important property of $\mathbf{B}_a$ which is sometimes observed and attributed to current channelling (Babour and Mosnier 1979) is its preferred direction of polarization, which in a strictly two-dimensional model would be perpendicular to the strike of the anomaly. The horizontal disturbance field $\mathbf{B}_a$ is plotted in figures 3 and 4 for northward and westward polarizations of the inducing magnetic field respectively.

2.2 *Anomalous current vectors*

The actual deformation of induced currents is visible in the anomalous currents $\mathbf{J}_a$

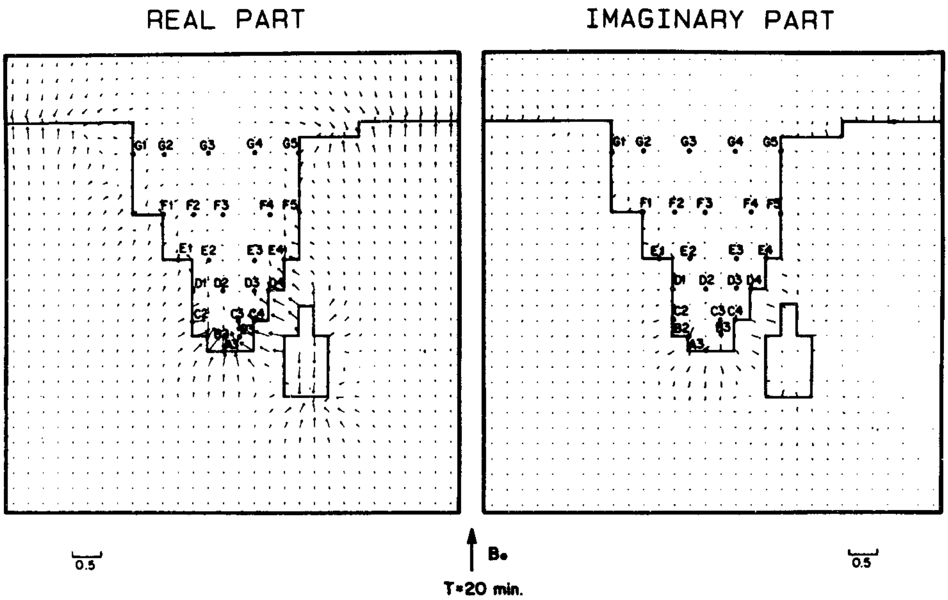

Figure 3. Horizontal disturbance vectors ($\mathbf{B}_a$) in the surface plane for a regional magnetic field of period $T=20$ minutes in the northward (positive x) direction. The arrows with pointed and flat heads respectively depict the in phase (Re $\mathbf{B}_a$) and quadrature (Im $\mathbf{B}_a$) components. ·

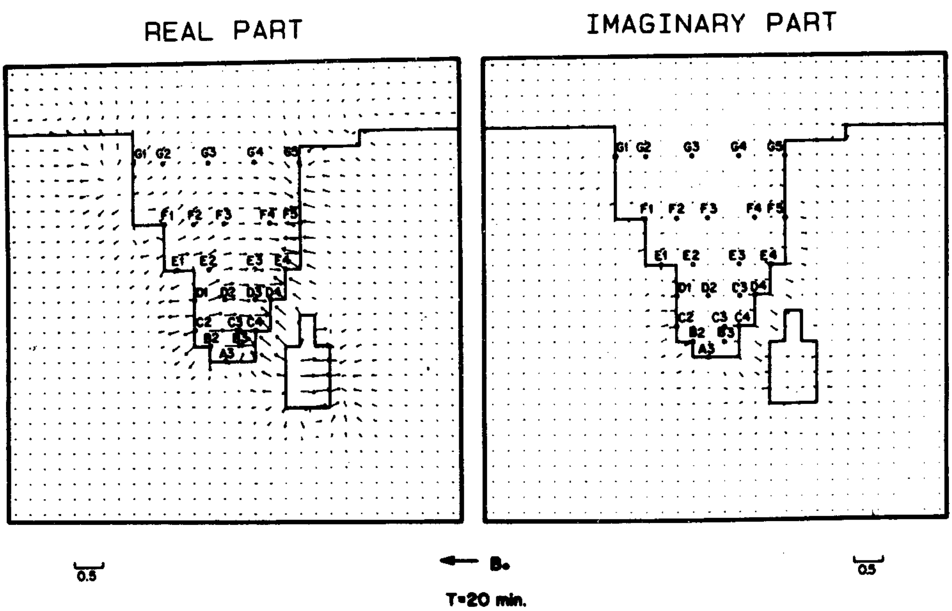

Figure 4. Same as in figure 3 but with the regional magnetic field in the westward (negative y) direction.

defined as (McKirdy and Weaver 1983)

$$\mathbf{J}_a = \mathbf{J} - \mathbf{J}_n, \tag{6}$$

$\mathbf{J}_n$ being the total current density at some 'normal' station N chosen to be well removed from the influence of oceans and other conductivity anomalies as shown in figure 2. Real and imaginary arrows indicating the direction and magnitude of $\mathbf{J}_a$ are drawn for the northwards (figure 5) and the westwards (figure 6) polarizations of the inducing field. The reader is reminded that the two-dimensional vector field depicted by these arrows is not solenoidal; sources or sinks of the surface currents arise from the vertical leakage out of or into the underlying medium (McKirdy and Weaver 1983).

2.3 *Equivalent current systems*

When rotated anti-clockwise through 90°, the vector $\mathbf{B}_a$ indicates the direction of, and is proportional to the magnitude of, the surface current density at that point of an equivalent system flowing in a thin sheet which must be superimposed in the westward or southward flow of unperturbed currents in order to give rise to the anomalous magnetic field $\mathbf{B}_a$ (Schmucker 1970 p. 23). This follows from the well-known boundary condition relating the discontinuity of the horizontal magnetic field across a thin sheet to the density of currents flowing in the sheet. Although such current systems are solenoidal, they do not represent the actual flow of induced currents. They are derived on the assumption that the surface sheet is isolated so that there is no electrical connection or mutual induction between it and an underlying structure, with the result, in particular, that vertical current leakage is completely inhibited.

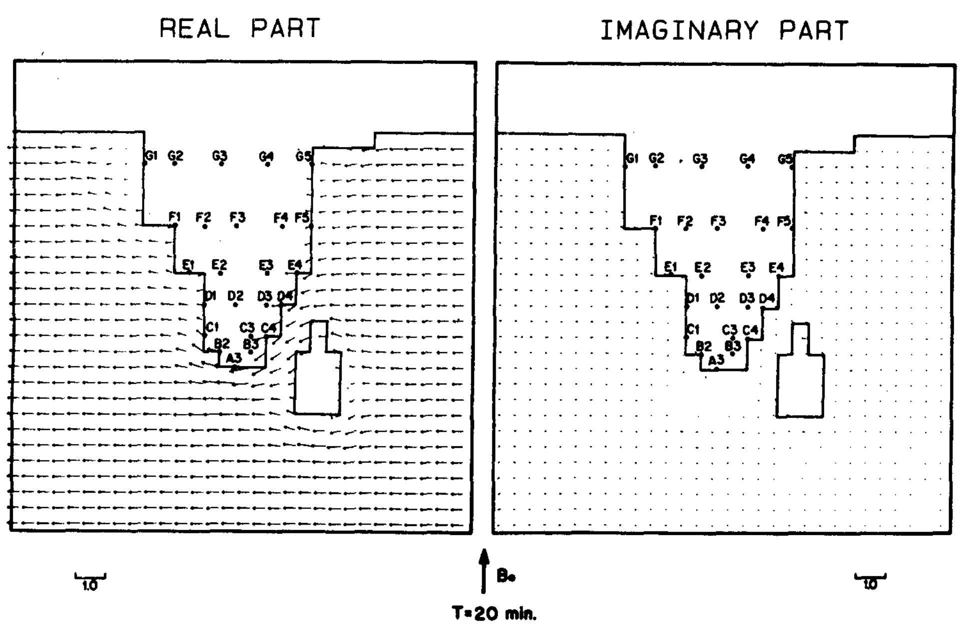

Figure 5. Anomalous current vectors ($\mathbf{J}_a$) in the surface plane for a regional magnetic field of period $T = 20$ minutes in the northward (positive x) direction. The arrows with pointed and flat heads respectively depict the in phase (Re $\mathbf{J}_a$) and quadrature (Im $\mathbf{J}_a$) components.

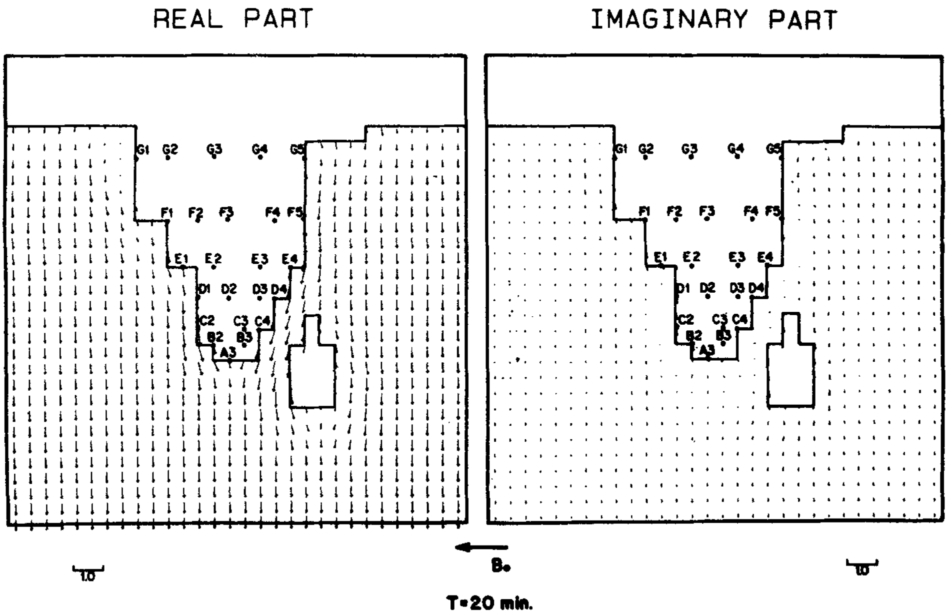

Figure 6. Same as figure 5 but with the regional magnetic field in the westward (negative y) direction.

Only if there were no substructure would the equivalent currents represent the true current system as stated by Weidelt (1977).

Nevertheless, such plots are very useful, a point emphasized by Jones (1983). An equivalent current system reveals the approximate pattern of toroidal currents in the sheet which produces the observed anomalous magnetic field, but excludes poloidal currents which have no external magnetic field associated with them. They therefore delineate more clearly the near-surface conductors, in contrast to the anomalous currents $\mathbf{J}_a$ which can be regarded more as indicators of vertical leakage, since they include the poloidal as well as the toroidal system. Equivalent current systems are plotted in figures 7 and 8 for northward and westward polarizations of the inducing field respectively.

2.4 *Apparent resistivity and phase*

These parameters are used to interpret magnetotelluric data and can be derived from the period-dependent impedance tensor $\mathbf{Z}$. The tensor elements define the linear relationship between the horizontal electric (U, V) and magnetic (H, D) field components given by

$$U = Z_{xx}H + Z_{xy}D,$$
$$V = Z_{yx}H + Z_{yy}D. \tag{7}$$

They can be obtained for our model from calculated field values for two different polarizations (e.g. for a northward and a westward inducing magnetic field). Once the elements of $\mathbf{Z}$ have been found in this way the horizontal north and east axes

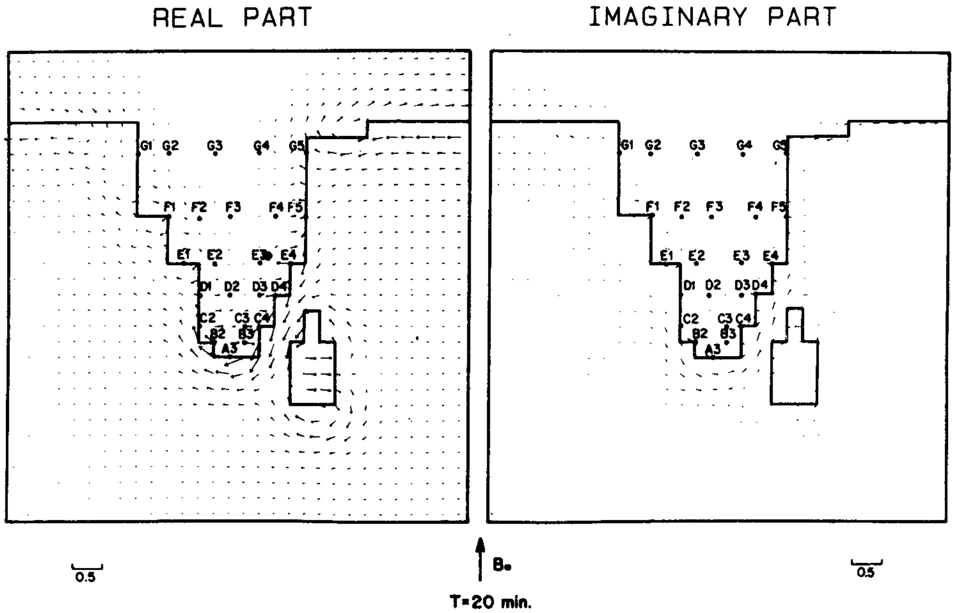

Figure 7. Equivalent current vectors obtained by rotating $\mathbf{B}_a$ anti-clockwise through 90° for a regional magnetic field of period $T = 20$ minutes in the northward (positive x) direction. The arrows with pointed and flat heads respectively depict the in phase and quadrature components.

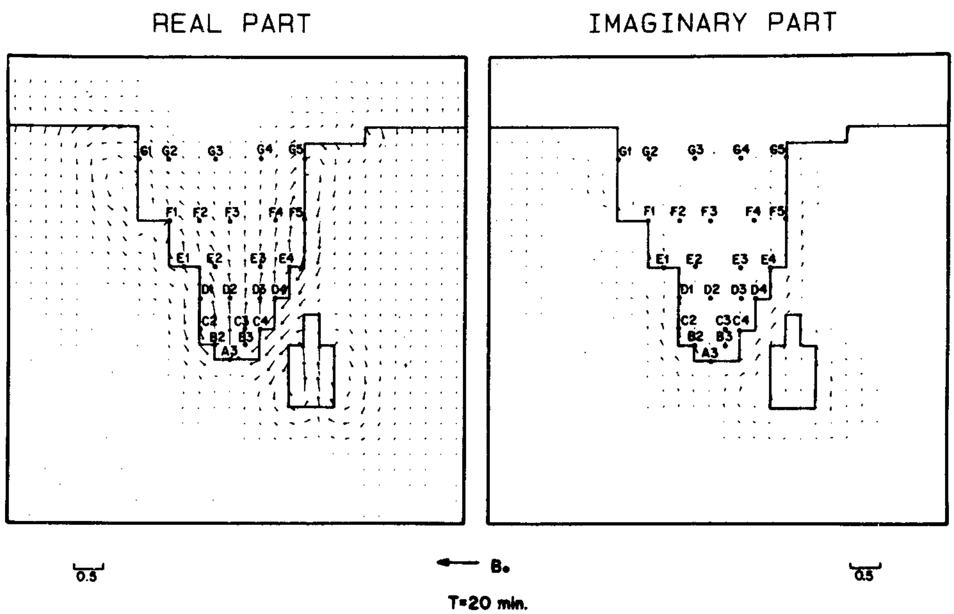

Figure 8. Same as figure 7 but with the regional magnetic field in the westward (negative y) direction.

(x, y) can be rotated clockwise from north through an angle θ so that the off-diagonal elements are maximized in some sense. It is usual to maximize the quantity $|Z_{xy}|^2 + |Z_{yx}|^2$ which gives

$$\theta = \frac{1}{4}\arctan\frac{Z_1 Z_2^* + Z_1^* Z_2}{Z_1 Z_1^* - Z_2 Z_2^*}, \tag{8}$$

where $Z_1 = Z_{xx} - Z_{yy}$ and $Z_2 = Z_{xy} + Z_{yx}$, and the asterisk denotes complex conjugate (Swift 1967). The new axes (x', y') are called the principal axes of $\mathbf{Z}$ and principal apparent resistivities ρ_1 and ρ_2 are defined with respect to these axes. The calculated values of these parameters at the array stations in the model are listed in table 1. The apparent resistivities are given in dimensionless units which can be converted into ohms by multiplying by $1/\sigma_1$ ($\sigma_1 = 0{\cdot}005$ S/m in our model). For a layered (one-dimensional) earth $Z_{xy} = -Z_{yx}$ and $Z_{xx} = Z_{yy} = 0$ so that ρ_1 is equal to ρ_2.

These parameters are very sensitive to the properties of the underlying layered structure, and are also influenced by complex geological structures and irregularities of coastlines that are impossible to model on a coarse grid. Thus it is not particularly meaningful to make a straight comparison of their calculated values with field data.

Table 1. Major and minor apparent resistivities (ρ_1, ρ_2), phases (ϕ_1, ϕ_2), and the azimuth (θ) of the major axis as calculated from the numerical model for the array stations. The azimuth (θ) of the major axis is measured clockwise from the north (x-direction of the model).

Station	Grid-point	ρ_1	ϕ_1	ρ_2	ϕ_2	θ
A3	(11, 15)	0·02	11°	0·01	15°	−82°
B2	(12, 14)	0·04	21°	0·02	24°	−52°
B3	(12, 16)	0·20	63°	0·07	67°	66°
C2	(13, 13)	0·02	15°	0·00	19°	−16°
C3	(13, 16)	0·24	58°	0·12	57°	−90°
C4	(13, 17)	0·03	19°	0·02	24°	32°
D1	(15, 13)	0·01	22°	0·01	12°	−4°
D2	(15, 15)	0·28	43°	0·11	59°	−89°
D3	(15, 17)	0·20	63°	0·07	54°	−61°
D4	(15, 18)	0·03	23°	0·02	23°	34°
E1	(17, 12)	0·03	28°	0·02	13°	−65°
E2	(17, 14)	0·28	63°	0·05	54°	69°
E3	(17, 17)	0·22	53°	0·07	59°	−61°
E4	(17, 19)	0·02	18°	0·02	16°	38°
F1	(20, 11)	0·05	25°	0·02	25°	36°
F2	(20, 13)	0·20	50°	0·09	59°	63°
F3	(20, 15)	0·09	65°	0·09	53°	−53°
F4	(20, 18)	0·27	46°	0·10	64°	−84°
F5	(20, 20)	0·01	14°	0·00	6°	4°
G1	(24, 9)	0·13	42°	0·08	54°	71°
G2	(24, 11)	0·13	56°	0·10	60°	82°
G3	(24, 14)	0·11	60°	0·10	63°	−53°
G4	(24, 17)	0·11	61°	0·09	50°	13°
G5	(24, 20)	0·08	33°	0·04	51°	−59°

Their relative values, however, do reveal trends, and suggest in a qualitative way how the oceans and other conductors included in our model affect the apparant resistivity and phase at individual stations.

3. Discussion

From figures 3 and 4 it is clear that the anomalous horizontal field is more pronounced on the east coast than on the west coast for both polarizations, which is in agreement with geomagnetic array data as represented by the substorm events of Thakur *et al* (1986), and is attributable to the effect of the channelling of induced currents along the Palk Strait at periods greater than 10 min (Singh *et al* 1982). In the case of the regional magnetic field oriented northwards, the real part of the anomalous H-component is positive (northwards) on the east coast, while the real D-component is negative (westwards) on the east coast but positive on the west coast. In the other polarization, when the regional field is westward in direction, the anomalous field on the east coast resembles that for the first polarization but on the west coast the real anomalous D-component has changed sign. (The imaginary vectors are small and make only small contributions to the total anomalous field.) The behaviour of the anomalous field vectors is perhaps more vividly portrayed by the equivalent current system in figures 7 and 8 which reveal the conducting paths followed by induced currents that give rise to the observed anomalous magnetic field. It is interesting to note that the direction of the anomalous horizontal field at ANN (E4) is oriented north-west which is in close agreement with the results obtained by Nityananda *et al* (1977) from an analysis of short-period events such as bays and SSCs. This direction seems to be characteristic of this zone as can be seen from the nature of perturbation vectors on both the east coast (E4, D4, C4) of India and the north-west coast of Sri Lanka.

At TRD (B_2), the direction of the horizontal anomalous vector for the northward polarization (figure 3) is slightly north of east (also at the next grid point further towards the east) which agrees with the trend of horizontal anomalies as reported by Nityananda *et al* (1977) at this permanent station for SSC events. For westward polarization (figure 4), the anomalous vector points southwards indicating a suppression in the H-component which contrasts with the small enhancement for the other polarization. It follows that events in which the inducing field is directed west of north will combine the effects of these two polarizations and could give a net suppression of the H component. This suppression in H at TRD has been observed by many authors (Singh *et al* 1982; Rajaram *et al* 1979; Nityananda *et al* 1977).

At inland stations it will be noted that the horizontal anomalous field is suppressed when the inducing field is polarized northwards, but in the westward polarization (negative D) this is not the case, the anomalous field being large and directed towards the east (positive D). Thus the anomalous field tends to cancel out the normal field in this latter polarization giving a smaller total D-field. The results agree, in general, with array data obtained by Thakur *et al* (1981, 1986).

Both the real and imaginary vectors near the Palk Strait in figures 3 and 4 show a preferred direction of polarization roughly perpendicular to the strait. This property of the vectors pertains only to this region and is not evident on the south or west coasts. It is clearly associated with channelling and confirms the existence of a preferred direction mentioned in § 2. The pattern of induced anomalous currents in figures 5 and 6 clearly demonstrates the deformation of current flow by the coastlines and the concentration of currents between India and Sri Lanka, as also noted by Takeda and Maeda (1979) from their model calculations, and by Papamastorakis and Haerendel (1983) from their analogue model experiment.

When the regional magnetic field is in the northward direction (figure 5), the real arrows depict the strong anomalous current flow in the east-west direction in the oceans. These regional currents flow south-west along the east coast, take a turn around the tip of peninsula and then northwards or north-west, before rejoining the east-west trend. The imaginary arrows, being small, do not exhibit any systematic current pattern.

In the other polarization (figure 6), the anomalous current flow in the ocean is towards the south and parallel to the coastline. The regional north-south induced currents also flow south-west in the Palk-Strait region, but flow south-east (i.e. opposite to east-west regional currents near TRD in figure 5) along the west coast. Again the imaginary arrows do not reveal any distinct current pattern.

It is evident from table 1 that for a period of 20 minutes both apparent resistivities and phases are nearly equal at the two inland stations F3 and G3 and calculations showed the skew to be very low there, suggesting that a one-dimensional model can provide a valid representation of the sub-surface conductivity structure at these stations. At other coastal and inland stations, however, there is a marked anisotropy, with both ρ_1 and ρ_2 generally small at the coastal stations. At inland stations, the direction of the principal axis defining the major apparent resistivity ρ_1 tends to be perpendicular to the nearest coastline, and is similar in this respect to an induction vector, as pointed out by Niblett *et al* (1987) from their study of geomagnetic data for the Alpha Ridge. On the other hand, at coastal stations close to regions of high conductance (i.e. all except F1, G1 and G5) the direction of the principal axis defining ρ_1 tends to be aligned more along the coast rather than perpendicular to it. This feature was also noted by Weaver (1982) at one of the coastal stations when modelling a region of northern and central Scotland. It may be concluded that at all array stations, except possibly F3 and G3, a two- or three-dimensional interpretation of magnetotelluric data will be required before a suitable depth-conductivity profile can be found.

In conclusion, we note that the above results have been obtained without including in our model the speculative anomaly between stations F3 and F4 proposed by Thakur *et al* (1986). Clearly the existence of such an anomaly would modify the calculated results in the neighbourhood of these stations.

Acknowledgements

This work was supported by research grants from the Natural Sciences and Engineering Research Council of Canada and the University of Victoria. Useful discussions with Professor B P Singh of the Indian Institute of Geomagnetism, Bombay, India while on his visit to the University of Victoria in August 1987 are gratefully acknowledged.

References

Agarwal A K and Weaver J T 1989 *Phys. Earth Planet. Inter.* **54** 320
Agarwal A K and Weaver J T 1990 *Phys. Earth Planet. Inter.* **60** 1
Babour K and Mosnier J 1979 *Geophys. J. R. Astron. Soc.* **36** 135
Burke K and Dewey J F 1973 *J. Geol.* **81** 406
Jones A G 1983 *Geophys. Surv.* **6** 79
Kunaratnam K 1987 *Phys. Earth Planet. Inter.* **49** 343
Mareschal M, Vasseur G, Srivastava B J and Singh R N 1987 *Phys. Earth Planet. Inter.* **45** 137
Mckirdy D McA and Weaver J T 1983 *J. Geomag. Geoelectr.* **35** 623
Mckirdy D McA, Weaver J T and Dawson T W 1985 *Geophys. J. R. Astron. Soc.* **80** 177
Niblett E R, Kurtz R D and Michaud C 1987 *Phys. Earth Planet. Inter.* **45** 101
Nityananda N, Agarwal A K and Singh B P 1977 *Phys. Earth Planet. Inter.* **15** p5
Nityananda N and Jayakumar D 1981 *Phys. Earth Planet. Inter.* **27** 223
Papamastorakis J and Haerendel G 1983 *J. Geophys.* **52** 61
Rajaram M, Singh B P, Nityananda N and Agarwal A K 1979 *Geophys. J. R. Astron. Soc.* **56** 127
Ramaswamy V, Agarwal A K and Singh B P 1985 *Phys. Earth Planet. Inter.* **39** 52
Schmucker U 1970 *Bull. Scripps Inst. Oceanogr.* **13**
Singh B P, Agarwal A K and Carlo L 1982 *J. Atmos. Terr. Phys.* **44** 241
Srivastava B J and Sanker Narayan P V 1967 *Proc. Symp. Upper Mantle Project*, National Geophysical Research Institute (India), Hyderabad p. 165
Swift C M 1967 *A magnetotelluric investigation of an electrical conductivity anomaly in the southwestern United States* Ph.D. Thesis, MIT Cambridge, Ma
Takeda M and Maeda H 1979 *J. Geophys.* **45** 209
Thakur N K, Mahashabde M V, Arora B R, Singh B P, Srivastava B J and Prasad S N 1981 *Geophys. Res. Lett.* **8** 947
Thakur N K, Mahashabde M V, Arora B R, Singh B P, Srivastava B J and Prasad S N 1986 *Geophys. J. R. Astron. Soc.* **86** 839
Vasseur G and Weidelt P 1977 *Geophys. J. R. Astron. Soc.* **51** 669
Weaver J T 1982 *Phys. Earth Planet. Inter.* **28** 161
Weidelt P 1977 *Acta. Geodact. Geophys. Montan.* **12** 195